J. Fluid Mech. (2019), *vol.* 878, *pp.* 169–189. © Cambridge University Press 2019
doi:10.1017/jfm.2019.644

Odd-viscosity-induced stabilization of viscous thin liquid films

E. Kirkinis[1],† **and A. V. Andreev**[1]

[1]Department of Physics, University of Washington, Seattle, WA 98195-1560, USA

(Received 25 March 2019; revised 1 August 2019; accepted 3 August 2019;
first published online 4 September 2019)

Thin viscous liquid films sitting on a solid substrate support nonlinear capillary waves, driven by surface shear stresses at a liquid–gas interface. When surface tension is spatially dependent other mechanisms, such as the thermocapillary effect, influence the dynamics of thin films. In this article we show that in liquids with broken time-reversal symmetry the character of the aforementioned waves and of the thermocapillary effect are significantly modified due to the presence of odd or Hall viscosity in the liquid. This is because odd viscosity gives rise to new terms in the pressure gradient of the flow thus modifying the evolution equation of the liquid–gas interface accordingly. These terms in turn break the reflection symmetry of the evolution equation leading the system to evolve from a pitchfork to a Hopf bifurcation. The odd-viscosity incipient waves can stabilize unstable thin liquid films. For instance, we show that they can suppress the thermocapillary instability. We establish the parameter ranges that odd viscosity has to satisfy in order to initiate those waves that will lead to stability.

Key words: thin films, capillary waves

1. Introduction

Stemming from early studies of the quantum Hall effect, Avron (1998) showed that apart from the well-known coefficient of viscosity, a classical liquid with broken time-reversal symmetry, either spontaneously or due to an external magnetic field or rotation, is endowed with a second viscosity coefficient termed odd or Hall viscosity. Such arguments had been put forward in the past in the context of plasmas (Lifshitz & Pitaevskii 1981) but only during the last few years have they received attention in the context of swimming strategies (Lapa & Hughes 2014), chiral active liquids (Banerjee *et al.* 2017) and the study of observable effects in incompressible liquids (Ganeshan & Abanov 2017). Chiral surface waves satisfying a complex Burgers' equation with imaginary viscosity have been found to exist even in the absence of gravity in such a liquid (Abanov, Can & Ganeshan 2018).

There are many instances in nature where the time-reversal symmetry of a classical liquid is broken, for instance in biological (Sumino *et al.* 2012), colloidal (Maggi *et al.* 2015) and granular systems (Tsai *et al.* 2005), and this new behaviour is expected to play a significant role in the dynamics of such systems, cf. Banerjee

† Email address for correspondence: kirkinis@uw.edu

https://doi.org/10.1017/jfm.2019.644 Published online by Cambridge University Press

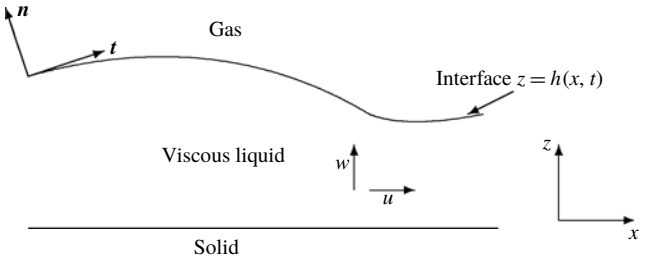


FIGURE 1. Geometry of the problem: a free interface at $z = h(x, t)$ with unit normal and tangent vectors $\boldsymbol{n}$ and $\boldsymbol{t}$ respectively, separates a gas phase from a viscous liquid (containing both even η^e and odd η^o viscosity coefficients) lying on a solid substrate. Here u and w are horizontal and vertical liquid velocities respectively. Dimensional quantities are denoted with lower case symbols here.

et al. (2017) and references therein. In addition, there are experimental observations in magnetic liquids (Chaves, Zahn & Rinaldi 2008) that cannot be explained by employing the classical theory of fluid flows. One such instance is the observation of interface patterns propagating in a direction opposite to the bulk liquid. Since time reversal is broken in such a system, it is expected that odd viscosity would play an important role.

In this article we consider a classical Newtonian liquid with broken time-reversal symmetry and an odd or Hall viscosity coefficient. We envision that this effect is caused by the presence of an external magnetic field which is for example applied radially in a cylinder of a liquid with a free surface. Then, the Cauchy stress tensor, apart from the rate-of-strain tensor, acquires additional terms that depend on field direction which break the time-reversal symmetry (Lifshitz & Pitaevskii 1981, § 13). By reducing the problem's geometry to two dimensions (see figure 1), thus considering the liquid sitting on a solid substrate and surrounded by an ambient gas phase in which the magnetic field is normal to the plane, we show that these new terms give rise to nonlinear viscous capillary waves that may lead to stabilization of an unstable film. We consider a thermocapillary system and show that odd viscosity can suppress the thermocapillary instability. These waves become prominent only when the shear surface stresses are spatially dependent. Two cases are developed in this article: surface stresses that arise due to the spatial variation of the surface tension (Oron, Davis & Bankoff 1997; Davis 2002) and surface shear that may arise from other sources such as blowing air (Davis, Gratton & Davis 2010) or applying a suitable temperature gradient (Kataoka & Troian 1999).

In § 2 we develop the theory of odd viscosity in the context of viscous thin liquid films by reducing the Navier–Stokes equations to a single partial differential equation describing the evolution of the liquid–gas interface. This reduction is possible by taking into account the long-wavelength approximation and retaining only the leading-order corrections (the lubrication approximation). Odd viscosity does not alter the shear stress but affects its normal counterpart at the free interface, in agreement with recent literature (Avron 1998; Lapa & Hughes 2014) where, for instance, a rotating disk experiences an additional pressure due to odd viscosity.

As a particular example in § 3 we employ a thermocapillary system (see figure 2) where interfacial shear stresses arise due to the variation of the surface tension σ with temperature ϑ. If this variation is represented by a linear law $\sigma - \sigma_0 \propto -(\vartheta - \vartheta_0)$

https://doi.org/10.1017/jfm.2019.644 Published online by Cambridge University Press

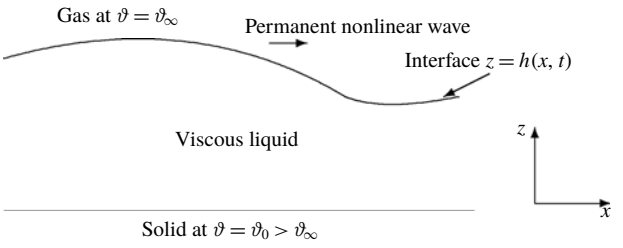


FIGURE 2. The thermocapillary effect: a free interface $z = h(x, t)$ separates a gas phase at temperature $\vartheta = \vartheta_\infty$ from a viscous liquid (containing both even η^e and odd η^o viscosity coefficients) lying on a solid substrate at temperature $\vartheta = \vartheta_0 > \vartheta_\infty$. Interfacial stresses arising from surface tension gradients, which in turn arise due to the temperature gradient, drive fluid from the hot depressions to the cool peaks leading to instability. The odd viscosity will give rise to wave propagation which, under certain circumstances, may lead to stabilization.

valid for common liquids (the subscript denotes reference values), then there is a surface flow from the hot to the cold end. Since bulk fluids are viscous they are dragged along; thus, interfacial temperature gradients induce bulk-liquid motion. This is the thermocapillary effect (Davis 1987; Oron *et al.* 1997; Davis 2002). In the presence of odd viscosity, this effect gives rise to spatially dependent shear stresses at the liquid–gas interface which in turn enter the pressure gradient and generate nonlinear non-dissipative capillary waves. These waves act in a stabilizing manner: the thermocapillary instability is suppressed and an interfacial pattern persists. We numerically solve the evolution equation to show the existence of these waves.

In § 4.1 a linear stability analysis leads to the dispersion relation for the waves whereby the odd-viscosity contribution is cubic with respect to the wavenumber. Analogous behaviour has been discussed before in the context of soliton dynamics of dispersive nature similar to the Kuramoto–Sivashinsky equation (Kawahara 1983; Kawahara & Toh 1988).

In § 5 we develop a mean-field theory to explain the reason behind the appearance of these waves. Solutions of the evolution equation of the liquid–gas interface are invariant with respect to the $O(2)$ symmetry group of translations and reflections when odd viscosity vanishes ($\eta^o \equiv 0$). A non-zero value of odd viscosity η^o on the other hand, breaks the $O(2)$ reflection symmetry and endows these systems with an $SO(2)$ symmetry such that solutions become invariant with respect to parallel translations only. This broken symmetry induces patterns that slowly drift in the frame of reference moving with velocity η^o. We perform a weakly nonlinear analysis of the evolution equation for an arbitrary value of the viscosity coefficient η^o to determine the velocity of the patterns and investigate the stability of the Hopf bifurcation. We establish the conditions under which odd viscosity gives rise to stabilization of an unstable film.

The presence of the magnetic field endows the heat flux with additional terms that depend on the temperature gradient and the field direction (Lifshitz & Pitaevskii 1981, § 13). However, for a sufficiently thin film where the long-wavelength approximation can be taken into account we show that the balance of energy reduces to well-known expressions found in the literature (Oron *et al.* 1997; Davis 2002). We include such a discussion in appendix A. In addition, by resorting to the full energy equation of a liquid we show that viscous heating arises only as a consequence of even viscosity and odd viscosity plays no role in the evolution of the entropy of the system, see

https://doi.org/10.1017/jfm.2019.644 Published online by Cambridge University Press

appendix B. In appendix C we derive the Landau equation for a thermocapillary system with odd viscosity. This result verifies the findings of the mean-field theory developed in § 5.

2. Odd viscosity in free surface viscous flows

Consider a two-dimensional thin liquid film (see figure 1) of thickness $h(x,t)$ sitting on a solid substrate surrounded by an ambient gas phase. In a liquid with broken time-reversal symmetry the Cauchy stress tensor $\boldsymbol{\sigma}$ consists of two parts:

$$\boldsymbol{\sigma} = \boldsymbol{\sigma}^e + \boldsymbol{\sigma}^o. \tag{2.1}$$

In two dimensions

$$\sigma^e_{ik} = -p\delta_{ik} + \eta^e\left(\frac{\partial u_i}{\partial x_k} + \frac{\partial u_k}{\partial x_i}\right), \quad i,k = 1,3, \tag{2.2}$$

is the standard (even) Cauchy stress tensor with standard (even) viscosity η^e and $\boldsymbol{\sigma}^o$ is the odd part of the Cauchy stress tensor which arises in the presence of time-reversal symmetry-breaking due, for instance, to a magnetic field. The general form of the odd stress tensor is characterized by several odd viscosity coefficients and depends on the orientation of the magnetic field (Lifshitz & Pitaevskii 1981, § 13), see also appendix A. We consider a planar flow in the x–z plane and assume that the magnetic field is perpendicular to it. In this case the odd part of the Cauchy stress tensor is characterized by a single odd viscosity coefficient and its components read (Avron 1998; Lapa & Hughes 2014)

$$\sigma^o_{ik} = -\eta^o(\delta_{i1}\delta_{k1} - \delta_{i3}\delta_{k3})\left(\frac{\partial u_1}{\partial x_3} + \frac{\partial u_3}{\partial x_1}\right) + \eta^o(\delta_{i1}\delta_{k3} + \delta_{i3}\delta_{k1})\left(\frac{\partial u_1}{\partial x_1} - \frac{\partial u_3}{\partial x_3}\right), \tag{2.3}$$

for $i,k = 1,3$, or explicitly, letting $u_1 = u$ and $u_3 = w$,

$$\sigma^o_{13} = \sigma^o_{31} = \eta^o(\partial_x u - \partial_z w) \quad \text{and} \quad \sigma^o_{33} = -\sigma^o_{11} = \eta^o(\partial_x w + \partial_z u), \tag{2.4a,b}$$

and η^o is the odd viscosity. We emphasize that in the presence of odd viscosity, the Cauchy stress tensor $\boldsymbol{\sigma}$ remains symmetric.

The Navier–Stokes equations become

$$\rho[u_t + uu_x + wu_z] = -p_x + \eta^e(u_{xx} + u_{zz}) - \eta^o(w_{xx} + w_{zz}) - \phi_x, \tag{2.5}$$

$$\rho[w_t + uw_x + ww_z] = -p_z + \eta^e(w_{xx} + w_{zz}) + \eta^o(u_{xx} + u_{zz}) - \phi_z, \tag{2.6}$$

where ϕ is a potential representing the effects of gravity, intermolecular forces or other fields.

At the liquid–gas interface $z = h(x,t)$, the shear and normal stresses are respectively

$$\boldsymbol{t\sigma n} = \frac{\partial \sigma}{\partial s} + \tau_0 \quad \text{and} \quad \boldsymbol{n\sigma n} = 2\kappa\sigma + \Pi, \quad \text{at} \quad z = h(x,t), \tag{2.7a,b}$$

where σ is the (variable) surface tension, s is arc length along the interface, κ the mean curvature of the surface, τ_0 is an external shear stress and Π an external normal stress on the boundary (Oron *et al.* 1997).

https://doi.org/10.1017/jfm.2019.644 Published online by Cambridge University Press

No-slip and no-penetration boundary conditions at the liquid–solid interface are expressed as

$$u = 0 \quad \text{and} \quad w = 0, \quad \text{at} \quad z = 0. \tag{2.8a,b}$$

The liquid–gas interface is described by the function $z = h(x, t)$ or, equivalently, the space curve $\boldsymbol{r}(x, t) = (x, h(x, t))$. The tangent and normal vectors to the interface are

$$\boldsymbol{t} = \frac{(1, h_x)}{\sqrt{1 + h_x^2}} \quad \text{and} \quad \boldsymbol{n} = \frac{(-h_x, 1)}{\sqrt{1 + h_x^2}}. \tag{2.9a,b}$$

The shear and normal components of the stress tensor on the liquid–gas interface are respectively

$$\boldsymbol{t}\boldsymbol{\sigma}\boldsymbol{n} = \frac{1}{1 + h_x^2}(1, h_x)\begin{pmatrix}\sigma_{11} & \sigma_{13}\\ \sigma_{31} & \sigma_{33}\end{pmatrix}\begin{pmatrix}-h_x\\ 1\end{pmatrix} = \frac{1}{1 + h_x^2}[\sigma_{13} - h_x^2\sigma_{31} + h_x(\sigma_{33} - \sigma_{11})] \tag{2.10}$$

and

$$\boldsymbol{n}\boldsymbol{\sigma}\boldsymbol{n} = \frac{1}{1 + h_x^2}(-h_x, 1)\begin{pmatrix}\sigma_{11} & \sigma_{13}\\ \sigma_{31} & \sigma_{33}\end{pmatrix}\begin{pmatrix}-h_x\\ 1\end{pmatrix} = \frac{1}{1 + h_x^2}[\sigma_{33} + h_x^2\sigma_{11} - h_x(\sigma_{13} + \sigma_{31})], \tag{2.11}$$

so that

$$\frac{1}{1 + h_x^2}[\sigma_{13} - h_x^2\sigma_{31} + h_x(\sigma_{33} - \sigma_{11})] = \frac{\partial\sigma}{\partial s} + \tau_0 \tag{2.12}$$

and

$$\frac{1}{1 + h_x^2}[\sigma_{33} + h_x^2\sigma_{11} - h_x(\sigma_{13} + \sigma_{31})] = 2\kappa\sigma + \Pi, \tag{2.13}$$

at the liquid–gas interface $z = h(x, t)$. Equation (2.12) is the shear stress condition and (2.13) the Laplace condition of normal stress balance at the liquid–gas interface. Also, $2\kappa = h_{xx}/(1 + h_x)^{3/2}$. To the above one may add the kinematic condition

$$w = h_t + uh_x, \tag{2.14}$$

at the liquid–gas interface.

Considering first the even-viscosity contributions we have (Oron *et al.* 1997; Davis 2002)

$$\boldsymbol{t}\boldsymbol{\sigma}^e\boldsymbol{n} = \frac{1}{1 + h_x^2}\eta^e[(-u_x + w_z)h_x + \eta^e(1 - h_x^2)(w_x + u_z)] \tag{2.15}$$

and

$$\boldsymbol{n}\boldsymbol{\sigma}^e\boldsymbol{n} = \frac{1}{1 + h_x^2}[-p + 2\eta^e w_z - 2\eta^e h_x(w_x + u_z) + h_x^2(-p + 2\eta^e u_x)]. \tag{2.16}$$

On the other hand, the contribution of the odd viscosity to the shear and normal stress is

$$\boldsymbol{t}\boldsymbol{\sigma}^o\boldsymbol{n} = \frac{1}{1 + h_x^2}\eta^o[(u_x - w_z)(1 - h_x^2) + 2h_x(w_x + u_z)] \tag{2.17}$$

and

$$\boldsymbol{n}\boldsymbol{\sigma}^o\boldsymbol{n} = \frac{1}{1 + h_x^2}\eta^o[(w_x + u_z)(1 - h_x^2) - 2h_x(u_x - w_z)], \tag{2.18}$$

respectively.

https://doi.org/10.1017/jfm.2019.644 Published online by Cambridge University Press

2.1. *Lubrication approximation*

In this approximation the Navier–Stokes equations are scaled with respect to a long wavelength λ which is a natural consequence of the longitudinal and vertical disparity of scales embodied in a thin liquid film. This introduces slow longitudinal and temporal variables

$$X=\frac{2\pi x}{\lambda}=\epsilon\frac{x}{h_0},\quad Z=\frac{z}{h_0}\quad\text{and}\quad T=\frac{2\pi U_0}{\lambda}t,\quad\text{for}\quad\epsilon=\frac{2\pi h_0}{\lambda},\tag{2.19a–c}$$

where h_0 and U_0 are characteristic scales for the liquid-film thickness and longitudinal velocity respectively and the partial derivatives $\partial/\partial X$ and $\partial/\partial Z$ are now quantities of unit order (Davis 2002). The velocity, pressure and liquid–gas interface location become respectively

$$U=\frac{u}{U_0},\quad W=\frac{\lambda}{2\pi h_0}\frac{w}{U_0}=\frac{1}{\epsilon}\frac{w}{U_0},\quad P=\frac{2\pi h_0}{\lambda}\frac{h_0 p}{\eta^e U_0},\quad H=\frac{h}{h_0}.\tag{2.20a–d}$$

We define the dimensionless Reynolds and scaled capillary numbers and potential:

$$Re=\frac{U_0 h_0\rho}{\eta^e},\quad \bar{C}=\epsilon^{-3}\frac{U_0\eta^e}{\sigma},\quad \Phi=\frac{\epsilon h_0\phi}{\eta^e U_0}.\tag{2.21a–c}$$

With the above notation, equations (2.5) and (2.6) obtain the following dimensionless form:

$$\epsilon\, Re\frac{\mathrm{D}U}{\mathrm{D}T}=-P_X+(\epsilon^2U_{XX}+U_{ZZ})-\frac{\eta^o}{\eta^e}\epsilon(\epsilon^2W_{XX}+W_{ZZ})-\Phi_X,\tag{2.22}$$

$$\epsilon^2 Re\frac{\mathrm{D}W}{\mathrm{D}T}=-\frac{P_Z}{\epsilon}+\epsilon(\epsilon^2W_{XX}+W_{ZZ})+\frac{\eta^o}{\eta^e}(\epsilon^2U_{XX}+U_{ZZ})-\frac{1}{\epsilon}\Phi_Z,\tag{2.23}$$

where $\mathrm{D}U/\mathrm{D}T=U_T+UU_X+WU_Z$ and $\mathrm{D}W/\mathrm{D}T=W_T+UW_X+WW_Z$.

The shear and normal components of the stress tensor from relations (2.15)–(2.18) become

$$\boldsymbol{t}\boldsymbol{\sigma}^e\boldsymbol{n}=\frac{\eta^e U_0}{h_0}\frac{1}{1+\epsilon^2H_X^2}[\epsilon(-U_X+W_Z)\epsilon H_X(1-\epsilon^2H_X^2)(\epsilon^2W_X+U_Z)],\tag{2.24}$$

$$\boldsymbol{n}\boldsymbol{\sigma}^e\boldsymbol{n}=\frac{1}{1+\epsilon^2H_X^2}\left[-p+2\eta^e\frac{\epsilon U_0}{h_0}W_Z-2\frac{\epsilon U_0}{h_0}\eta^eH_X(U_Z-\epsilon^2W_X)+\epsilon^2H_X^2\left(-p+2\eta^e\frac{\epsilon U_0}{h_0}\epsilon U_X\right)\right],\tag{2.25}$$

$$\boldsymbol{t}\boldsymbol{\sigma}^o\boldsymbol{n}=\frac{\eta^o U_0}{h_0}\frac{1}{1+\epsilon H_X^2}[\epsilon(U_X-W_Z)(1-\epsilon H_X^2)+2\epsilon H_X(\epsilon^2W_X+U_Z)]\tag{2.26}$$

and

$$\boldsymbol{n}\boldsymbol{\sigma}^o\boldsymbol{n}=\frac{\eta^o U_0}{h_0}\frac{1}{1+\epsilon H_X^2}[(\epsilon^2W_X+U_Z)(1-\epsilon H_X^2)-2\epsilon^2H_X(U_X-W_Z)].\tag{2.27}$$

The kinematic condition (2.14) becomes $W=H_T+UH_X$ and leads to the following evolution equation for the liquid–gas profile H:

$$H_T+\left[\int_0^H U\,\mathrm{d}Z\right]_X=0.\tag{2.28}$$

https://doi.org/10.1017/jfm.2019.644 Published online by Cambridge University Press

This is obtained in the standard way (Oron *et al.* 1997) by integrating the incompressibility condition $U_X + W_Z = 0$ from $Z = 0$ to $Z = H(X, T)$, using (2.8*b*) and integration by parts.

We proceed by expanding all fields in a regular perturbation expansion with respect to the small parameter ϵ: $(U, W, P) = (U^0, W^0, P^0) + \epsilon(U^1, W^1, P^1) + O(\epsilon^2)$. To leading order (which corresponds to the lubrication approximation) and dropping superscripts denoting order in ϵ, the scaled equations (2.22)–(2.23) simplify to

$$-\Phi_X - P_X + U_{ZZ} = 0, \quad -P_Z - \Phi_Z = 0. \tag{2.29a,b}$$

The boundary conditions (2.8) become

$$U = 0, \quad W = 0, \quad \text{at} \quad Z = 0. \tag{2.30a,b}$$

Introducing the dimensionless surface shear and surface tension

$$\tau = \frac{h_0 \tau_0}{\eta^e U_0} \quad \text{and} \quad \Sigma = \frac{\epsilon \sigma}{\eta^e U_0}, \tag{2.31a,b}$$

respectively, we obtain the expressions for the sought shear stress by employing (2.7*a*) (through (2.24) and (2.26))

$$U_Z = \tau + \Sigma_X. \tag{2.32}$$

Equation (2.32) is identical to the one found in the literature of thin liquid films when only even viscosity is present (Oron *et al.* 1997).

From (2.7*b*) (through (2.25) and (2.27)) the normal stress reads

$$-P + \frac{\eta^o}{\eta^e} U_Z = \bar{C}^{-1} H_{XX}, \tag{2.33}$$

where for simplicity we have set the normal stress at the boundary $\Pi \equiv 0$. Equation (2.33) shows that the presence of odd viscosity leads to an extra term in the normal boundary condition proportional to the velocity gradient U_Z. This is the expected behaviour since it is known from the literature (Avron 1998; Lapa & Hughes 2014) that the effect of odd viscosity on a rotating disk is to apply a normal pressure. We may define its reduced counterpart (Oron *et al.* 1997; Davis 2002)

$$\bar{P} = P + \Phi = \Phi|_{Z=H} + \frac{\eta^o}{\eta^e} U_Z|_{Z=H} - \bar{C}^{-1} H_{XX}. \tag{2.34}$$

Integration of (2.29*b*) and application of the normal stress boundary condition (2.34) leads to the velocity distribution in the long-wavelength approximation (cf. Oron *et al.* (1997) equation (2.26))

$$U(X, Z, T) = (\tau + \Sigma_X) Z + \bar{P}_X \left(\tfrac{1}{2} Z^2 - HZ \right), \tag{2.35}$$

where (2.32) and (2.34) lead to

$$\bar{P}_X = \Phi_X|_{Z=H} + \frac{\eta^o}{\eta^e} (\tau + \Sigma_X)_X - \bar{C}^{-1} H_{XXX}. \tag{2.36}$$

The sought evolution equation for the liquid–gas interface (2.28) with the velocity profile (2.35) and pressure gradient from (2.36) becomes

$$H_T + \left[\tfrac{1}{2} (\tau + \Sigma_X) H^2 - \tfrac{1}{3} \bar{P}_X H^3 \right]_X = 0. \tag{2.37}$$

Thus a non-zero odd viscosity η^o leads to new effects in the evolution of thin liquid films. For example, thermocapillary flow with surface tension gradient Σ_X, in addition to the well-known thinning and rupture of a thin liquid film, also leads to nonlinear capillary wave propagation. This case is analysed in the following sections.

https://doi.org/10.1017/jfm.2019.644 Published online by Cambridge University Press

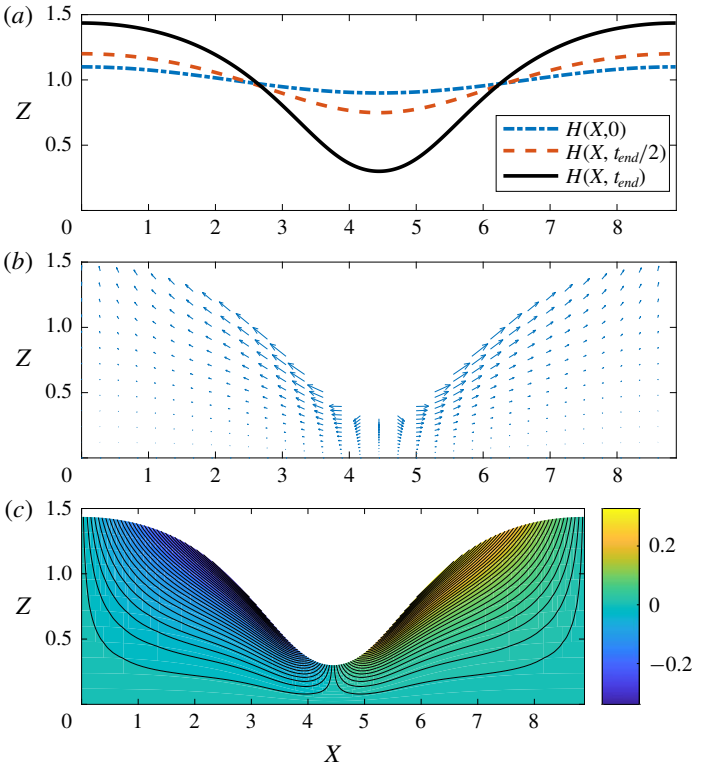


FIGURE 3. (Colour online) Surface tension gradients induced by temperature gradients lead to thinning of depressions in a thin liquid film without odd viscosity ($\eta^o = 0$). Numerical solutions of the thin-film equation (3.15) with surface tension gradient Σ_X from (3.14). (*a*) Snapshots of the gas–liquid interface of a liquid film towards rupture. (*b*) Velocity field at time t_{end}. (*c*) Streamlines at time t_{end}.

3. Thermocapillary flow with odd viscosity

Consider a two-dimensional thin liquid film (cf. figure 2) of thickness $h(x, t)$ on a solid substrate surrounded by an ambient gas phase where interfacial shear stresses arise due to the variation of the surface tension σ with temperature ϑ.

Thermocapillary instabilities arise because a corrugated interface in a fixed temperature gradient experiences hot regions at valleys and cool regions at peaks. The thermocapillary effect drives interfacial fluid from depressions to peaks and since the liquid is viscous, bulk fluid as well, see figure 3. This leads to film rupture and substrate dewetting (Oron *et al.* 1997; Davis 2002).

For an incompressible liquid the conservation of energy is given by (cf. Landau & Lifshitz (1987) § 50)

$$\rho c_p(\vartheta_t + u\vartheta_x + w\vartheta_z) = k_{th}\nabla^2\vartheta, \tag{3.1}$$

where c_p is the specific heat at constant pressure and k_{th} is the thermal conductivity of the liquid.

The boundary conditions for a thermocapillary system are

$$\vartheta = \vartheta_0 \quad \text{at} \quad z = 0 \quad \text{and} \quad k_{th}\boldsymbol{n}\cdot\nabla\vartheta + \alpha_{th}(\vartheta - \vartheta_\infty) = 0, \quad \text{at} \quad z = h(x, t), \tag{3.2a,b}$$

https://doi.org/10.1017/jfm.2019.644 Published online by Cambridge University Press

where ϑ_0 is the temperature of the rigid plane, ϑ_∞ the temperature of the gas phase and α_{th} the heat transfer coefficient describing the rate of heat transfer from the liquid to the ambient gas phase (Oron *et al.* 1997; Davis 2002). We note that in the presence of a magnetic field the energy equation (3.1) and boundary conditions (3.2) are endowed with additional terms (see appendix A). In the long-wavelength approximation these terms are of higher order with respect to the perturbation parameter ϵ and they are not pursued further here. For certain system parameter regimes, viscous heating terms in (3.1) (Kirkinis & Andreev 2019) may also become important. In this article we neglect such contributions as this is customary in the thin liquid film literature (Oron *et al.* 1997; Davis 2002).

We now introduce the dimensionless temperature

$$\Theta(X, Z, T) = \frac{\vartheta - \vartheta_\infty}{\vartheta_0 - \vartheta_\infty}, \tag{3.3}$$

as well as the dimensionless Prandtl and Biot numbers

$$Pr = \frac{\eta^e c_p}{k_{th}}, \quad B = \frac{\alpha_{th} h_0}{k_{th}}. \tag{3.4a,b}$$

With these dimensionless quantities, the energy equation (3.1) and boundary conditions (3.2) become respectively (Oron *et al.* 1997; Davis 2002)

$$\epsilon Re Pr(\Theta_T + U\Theta_X + W\Theta_Z) = \epsilon^2 \Theta_{XX} + \Theta_{ZZ} \tag{3.5}$$

and

$$\Theta = 1 \quad \text{at} \quad Z = 0 \quad \text{and} \quad \Theta_Z - \epsilon^2 \Theta_X H_X + B\Theta(1 + \epsilon^2 H_X^2)^{1/2} = 0 \quad \text{at} \quad Z = H. \tag{3.6a,b}$$

Employing the long-wavelength approximation and considering the leading-order correction (the lubrication approximation), energy equation (3.5) and boundary conditions (3.6*a*,*b*) become respectively

$$\Theta_{ZZ} = 0 \tag{3.7}$$

and

$$\Theta = 1 \quad \text{at} \quad Z = 0, \quad \Theta_Z + B\Theta = 0 \quad \text{at} \quad Z = H(X, T). \tag{3.8a,b}$$

Other dimensionless parameters employed in the subsequent analysis are the gravity number G and the Marangoni number M:

$$G = \epsilon \frac{\rho g h_0^2}{\eta^e U_0}, \quad M = \frac{\Delta\sigma}{\eta^e U_0}\epsilon, \tag{3.9a,b}$$

where $\Delta\sigma$ is the variation of surface tension over the temperature domain $\Delta\vartheta = \vartheta_0 - \vartheta_\infty$ so that

$$\Delta\sigma = \gamma \Delta\theta. \tag{3.10}$$

Equation (3.10) is derived from the equation of state approximated by a linear law

$$\sigma = \sigma_0 - \gamma(\vartheta - \vartheta_0), \tag{3.11}$$

where γ is positive for common liquids (Oron *et al.* 1997; Davis 2002).

Equation (3.7) leads to the well-known form of the temperature distribution (Oron *et al.* 1997; Davis 2002)

$$\Theta(X, Z, T) = 1 - \frac{BZ}{1 + BH}. \tag{3.12}$$

https://doi.org/10.1017/jfm.2019.644 Published online by Cambridge University Press

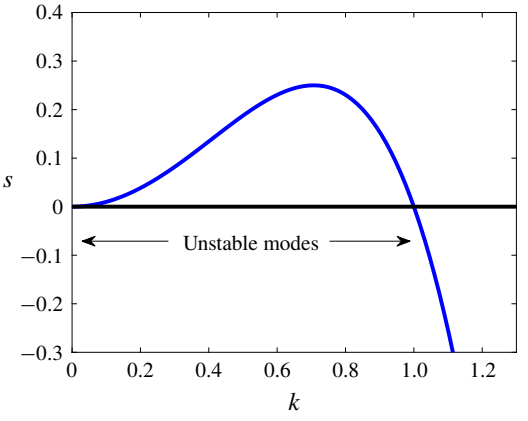


FIGURE 4. (Colour online) Growth rate $s = k^2 - k^4$ obtained from linear stability analysis (Oron *et al.* 1997; Davis 2002) of the thin-film evolution equation (3.15) showing the band of unstable wavenumbers $0 < k < k_{cr} = 1$.

3.1. *Evolution equation for the liquid–gas interface*

We thus need to calculate Σ_X. This can be done by considering the variation of the surface tension at the liquid–gas interface, that is, $\Sigma = \Sigma(\Theta(H))$. The chain rule leads to

$$\Sigma_X = \frac{\mathrm{d}\Sigma}{\mathrm{d}\Theta}\left[\frac{\partial\Theta}{\partial X}\right]. \tag{3.13}$$

As is common in the literature we set $\mathrm{d}\Sigma/\mathrm{d}\Theta = -M$, where M is the Marangoni number. We thus obtain that

$$\Sigma_X = \frac{BMH_X}{(1+BH)^2}, \tag{3.14}$$

which is the standard result obtained in the literature (Oron *et al.* 1997; Davis 2002). Thus, our aim is to solve the evolution equation (2.37) with the surface tension gradient given by (3.14), that is, solve

$$H_T + \tau HH_X + \left[\frac{1}{2}\Sigma_X H^2 - \frac{1}{3}\left(\frac{\eta^o}{\eta^e}\Sigma_{XX} + GH_X - \bar{C}^{-1}H_{XXX}\right)H^3\right]_X = 0. \tag{3.15}$$

In the subsequent discussion we will consider a constant surface shear τ so only the surface tension gradient will appear in the expression for the pressure.

4. Stability analysis

4.1. *Linear stability*

Following the standard linear stability analysis of Oron *et al.* (1997) and Davis (2002) by substituting $H = 1 + \delta \mathrm{e}^{sT+\mathrm{i}(kX-\omega T)}$ into (3.15) (assuming that s and ω are real and $\delta \ll 1$) we obtain the growth rate and frequency

$$s = \left[\frac{MB}{2(1+B)^2} - \frac{G}{3}\right]k^2 - \frac{1}{3\bar{C}}k^4, \quad \omega = \tau k + \frac{k^3}{3}\frac{\eta^o}{\eta^e}\frac{BM}{(1+B)^2}, \tag{4.1a,b}$$

https://doi.org/10.1017/jfm.2019.644 Published online by Cambridge University Press

respectively. Thus, there is a band of unstable wavenumbers $0 < k < k_{cr}$ whose critical value k_{cr} for the onset of instability is found when s becomes positive, that is, when

$$k_{cr}^2 = \frac{3MB\bar{C}}{2(1+B)^2} - \bar{C}G. \tag{4.2}$$

This requires that the Marangoni number M exceeds its critical value

$$M_{cr} = \frac{2G(1+B)^2}{3B}. \tag{4.3}$$

For values $M = 4(1+B)^2/B, G = 3, \bar{C} = 1/3$ we obtain the critical wavenumber $k_{cr} = 1$ and the band of unstable wavenumbers $0 < k < 1$, see figure 4.

The wavenumber dependence of the frequency ω in (4.1) is suggestive of the effectiveness of odd viscosity in stabilizing a film. Because odd viscosity is associated with cubic terms of wavenumber it is expected that stabilization will take place only at high wavenumbers.

5. Travelling waves in odd-viscosity liquids

5.1. *O*(2) *and SO*(2) *symmetries of the thin-film equations*

In the absence of odd viscosity ($\eta^o \equiv 0$) and surface shear ($\tau \equiv 0$) the thin-film equation (3.15) is invariant under the group $O(2)$ of parallel translations and reflections

$$\Pi_1 : X \to X + X_0, \quad \Pi_2 : X \to -X. \tag{5.1a,b}$$

If an external mechanism such as a magnetic field becomes operative, time-reversal breaks and odd viscosity becomes prominent. Non-vanishing odd viscosity or surface shear gives rise to a new term in the thin-film equation (3.15) (second or fourth term) that breaks the reflection (but not the parallel translation) symmetry. The surface shear term is of advective character and has been discussed before in the context of suppressing the van-der-Waals-driven rupture (Kirkinis & Davis 2015). The term associated with odd viscosity is of (nonlinearly) dispersive nature analogous to the dispersive Kuramoto–Sivashinsky equation (Kawahara 1983; Kawahara & Toh 1988).

5.2. *Broken symmetry*

At the threshold of instability, there is a subcritical pitchfork bifurcation, already discussed in the literature of thin liquid films (Erneux & Davis 1993). In this case the liquid–gas interface profile satisfying (3.15) has the form

$$H(X, T) = 1 + \delta Re\{A(T)e^{iqX}\} + O(\delta^2), \tag{5.2}$$

where q is the critical wavenumber and δ measures distance from criticality. The absence of odd viscosity ($\eta^o \equiv 0$) and surface shear ($\tau \equiv 0$) imparts the following properties onto the complex amplitude A:

$$\text{parallel translation} \quad \Pi_1 : X \to X + X_0, \quad A \to Ae^{iqX_0} \tag{5.3}$$

and

$$\text{reflection} \quad \Pi_2 : X \to -X, \quad A \to A^*. \tag{5.4}$$

https://doi.org/10.1017/jfm.2019.644 Published online by Cambridge University Press

Thus, the amplitude equation is a Landau equation of the general form

$$A_T = \alpha_1 A + \alpha_2 A|A|^2, \tag{5.5}$$

for some constants α_i that in general depend on the wavenumber q at the onset of instability. When $\alpha_2 > 0$ the resulting equilibria correspond to a subcritical pitchfork (Cross & Hohenberg 1993, p. 867). In polar coordinates where $A = Re^{i\theta}$ (5.5) can be expressed as $R_T = \alpha_1 R + \alpha_2 R^3$ and $\theta_T = 0$.

In the presence of odd viscosity or surface shear, either of the terms $\frac{1}{2}[H^2 \Sigma_{XX}]_X$ or $\tau H H_X$ breaks the reflection symmetry of (3.15) and the Landau equation acquires complex coefficients

$$A_T = (\alpha_1 + i\beta_1 \eta^o)A + (\alpha_2 + i\beta_2 \eta^o)A|A|^2, \tag{5.6}$$

for some constants α_i and β_i which, in general, depend on η^o (or τ). In polar coordinates the phase of (5.6) can be expressed as $\theta_T = \eta^o(\beta_1 + \beta_2 R^2)$. Now, the resulting equilibria correspond to a Hopf bifurcation which implies travelling wave solutions of the thin-film equation (3.15).

5.3. *Mean-field analysis*

We perform a mean-field analysis of (3.15) for an arbitrary value of the odd viscosity η^o in the vicinity of the onset of instability following the arguments developed by Kirkinis & Davis (2015). We introduce a Galilean frame of reference $\xi = X - VT$ moving with velocity V. Substituting into (3.15) and performing one integration we obtain

$$-VH + \frac{1}{2}(\tau + \Sigma_\xi)H^2 - \frac{1}{3}\left(\frac{\eta^o}{\eta^e}\Sigma_{\xi\xi} + GH_\xi - \bar{C}^{-1}H_{\xi\xi\xi}\right)H^3 = K, \tag{5.7}$$

where K is an integration constant.

We expand K and M in a perturbation series or equivalently K and the bifurcation parameter

$$a = \frac{M - M_{cr}}{M_{cr}}, \tag{5.8}$$

where $M_{cr} = (2/3)G(1+B)^2/B$ is the critical Marangoni number. Thus,

$$(V, K, a) = (V_0, K_0, a_0) + \delta(V_1, K_1, a_1) + \delta^2(V_2, K_2, a_2) + O(\delta^3), \tag{5.9}$$

and expand H about a steady state

$$H = 1 + \delta(A_c \cos q\xi + A_s \sin q\xi) + \delta^2(B_c \cos 2q\xi + B_s \sin 2q\xi) + O(\delta^2), \tag{5.10}$$

for real amplitudes A_c, B_c etc. and wavenumber q associated with the primary bifurcation. Here δ denotes distance from criticality.

To leading order in δ we find

$$V_0 = \frac{2(\bar{C}G + q^2)q^2}{9\bar{C}}\frac{\eta^o}{\eta^e} + \tau, \quad K_0 = -V_0 + \frac{\tau}{2} \quad \text{and} \quad a_0 = \frac{q^2}{\bar{C}G}. \tag{5.11a–c}$$

https://doi.org/10.1017/jfm.2019.644 Published online by Cambridge University Press

V_0 and a_0 are the standard results of linear stability analysis (Oron *et al.* 1997). For instance, V_0 can be derived by substituting into ω (4.1) the Marangoni number from (4.2). The first-order corrections vanish and, to second order, we obtain

$$\begin{aligned} a_2 \;=\; & -\frac{9({A_c}^2+{A_s}^2)}{4\bar{C}\left((\bar{C}G+q^2)^2\left(\frac{\eta^o}{\eta^e}\right)^2+9q^2\right)G(B+1)^2} \\ & \times\left(\frac{1}{27}(\bar{C}G+q^2)^2(27B^2\bar{C}G+35\,B^2q^2+42B\bar{C}G+30Bq^2+12\bar{C}G-24q^2)\left(\frac{\eta^o}{\eta^e}\right)^2\right. \\ & +\frac{1}{12q^2}\bar{C}(B+1)(\bar{C}G+q^2)(9B\bar{C}G+5Bq^2+3\bar{C}G-21q^2)\tau\frac{\eta^o}{\eta^e}-\frac{3}{4q^2}C^2\tau^2(B+1)^2 \\ & \left.+\,(\bar{C}G+q^2)\left(\frac{3}{2}B^2\bar{C}G+B\bar{C}G+\frac{1}{6}\bar{C}G+\frac{15}{2}\,B^2q^2+5Bq^2+\frac{7}{6}q^2\right)\right), \end{aligned} \tag{5.12}$$

$$\begin{aligned} V_2 \;=\; & -\frac{7({A_c}^2+{A_s}^2)}{\left(27(\bar{C}G+q^2)^2\left(\frac{\eta^o}{\eta^e}\right)^2+243q^2\right)(B+1)^2\bar{C}} \\ & \times\left(\frac{1}{7}\,q^2(\bar{C}G+q^2)^2(7\,B^2\bar{C}G+11\,B^2q^2+24\,B\bar{C}G+18\,Bq^2+15\,\bar{C}G-3\,q^2)\right. \\ & \times\left(\frac{\eta^o}{\eta^e}\right)^3+\frac{9\,\bar{C}(B+1)q^2(\bar{C}G+q^2)(5\,B\bar{C}G+4\,Bq^2+6\,\bar{C}G)\tau}{14q^2}\left(\frac{\eta^o}{\eta^e}\right)^2 \\ & +\frac{81\,\bar{C}^2(B+1)^2(\bar{C}G-q^2)\tau^2}{112q^2}\frac{\eta^o}{\eta^e}+\frac{243\,\bar{C}(B+1)q^2(3\,B\bar{C}G+9\,Bq^2+\bar{C}G+7\,q^2)\tau}{112q^2} \\ & \left.-\,\frac{(27\,B+9)(3\,B\bar{C}^2G^2-6\,B\bar{C}Gq^2-21\,Bq^4+\bar{C}^2G^2-18\,\bar{C}Gq^2-31\,q^4)}{56}\frac{\eta^o}{\eta^e}\right) \end{aligned} \tag{5.13}$$

and

$$K_2=-V_2+(A_c^2+A_s^2)\left(\frac{(\bar{C}G+q^2)q^2}{3\bar{C}}\frac{\eta^o}{\eta^e}+\frac{\tau}{4}\right). \tag{5.14}$$

We recognize the last term in (5.12) as being the well-known correction (see equation (2.27) in Kirkinis & Davis (2015) by setting $\tau=0$) signifying the subcritical behaviour of the bifurcation, a subcritical pitchfork of revolution.

When $\eta^o=0$ (5.12) shows that there is a critical value τ_{cr} of the surface shear above which the Hopf bifurcation becomes supercritical

$$\tau_{cr}^2=\frac{2q^2(\bar{C}G+q^2)(9\,B^2\bar{C}G+45\,B^2q^2+6\,B\bar{C}G+30\,Bq^2+\bar{C}G+7\,q^2)}{9(B+1)^2\bar{C}^2}. \tag{5.15}$$

Similarly, when $\tau=0$ (5.12) shows that there is a critical value of odd viscosity η^o_{cr}

$$\left(\frac{\eta^o}{\eta^e}\right)^2_{cr}=\frac{-9(9\,B^2\bar{C}G+45\,B^2q^2+6\,B\bar{C}G+30\,Bq^2+\bar{C}G+7\,q^2)}{2(\bar{C}G+q^2)(27\,B^2\bar{C}G+35\,B^2q^2+42\,B\bar{C}G+30\,Bq^2+12\,\bar{C}G-24\,q^2)}, \tag{5.16}$$

https://doi.org/10.1017/jfm.2019.644 Published online by Cambridge University Press

	Silicon oil	Water
ϑ (°C)	25	60
ρ (g cm^{-3})	9.6×10^{-1}	9.83×10^{-1}
η^e (g cm^{-1} s^{-1})	4.8×10^{-1}	4.67×10^{-3}
c_p (g s^{-2} °C^{-1})	1.51×10^{7}	4.18×10^{7}
k_{th} (g cm s^{-3} °C^{-1})	1.51×10^{4}	6.51×10^{4}
σ (g s^{-2})	2.08×10^{1}	6.62×10^{1}
γ (g s^{-2} °C^{-1})	6.8×10^{-2}	1.74×10^{-1}
α_{th} (g s^{-3} °C^{-1})	1×10^{4}	1×10^{4}

TABLE 1. Experimental values taken from Tan, Bankoff & Davis (1990).

as long as the denominator in (5.16) is negative. This is ensured when

$$q^2 > -3\,\frac{\bar{C}G(9\,B^2 + 14\,B + 4)}{35\,B^2 + 30\,B - 24}, \tag{5.17}$$

which in turn sets an upper bound on the Biot number B

$$B < -\frac{3}{7} + \frac{\sqrt{1065}}{35} \sim 0.5. \tag{5.18}$$

This bound is consistent with the behaviour of common liquids (Oron *et al.* 1997). In the limit of small Biot number $B \to 0$ we require that

$$q^2 > \frac{\bar{C}G}{2}. \tag{5.19}$$

As expected then, from our discussion in § 4.1, only high-wavenumber perturbations to the free surface can be stabilized with odd viscosity.

The following three parameter regimes can be distinguished.

(i) When $(\tau, \eta^o) = (0, 0)$, a_2 is always negative (see the last term in (5.12)) and the film is unstable; it proceeds to rupture and leads to substrate dewetting. This corresponds to a subcritical bifurcation. This behaviour corresponds to the film snapshots in figure 3(*a*).

(ii) When $\eta^o = 0$ and $0 < \tau < \tau_{cr}$ or when $\tau = 0$ and $0 < \eta^o < \eta^o_{cr}$ subject to the condition (5.19), there is wave propagation but the film still ruptures albeit at a reduced rate; a_2 is still negative but approaches its zero value. The bifurcation is a subcrtitical Hopf.

(iii) When $\eta^o = 0$ and $\tau > \tau_{cr}$ or when $\tau = 0$ and $\eta > \eta^o_{cr}$ subject to the condition (5.19) there is wave propagation and the film reaches a stable steady state in the frame of reference moving with velocity V. This corresponds to a supercritical Hopf bifurcation. Figure 5 shows snapshots of the film propagating with velocity V. This behaviour corresponds to the film snapshots in figures 5(*a*) and 6(*a*).

Among these three cases one can find regimes where both parameters play a role in the stabilization of the liquid film. This behaviour corresponds to the film snapshots in figure 7(*a*).

To aid the reader, in appendix C we make a direct connection between the bifurcation criterion (5.12) and the Landau equation.

https://doi.org/10.1017/jfm.2019.644 Published online by Cambridge University Press

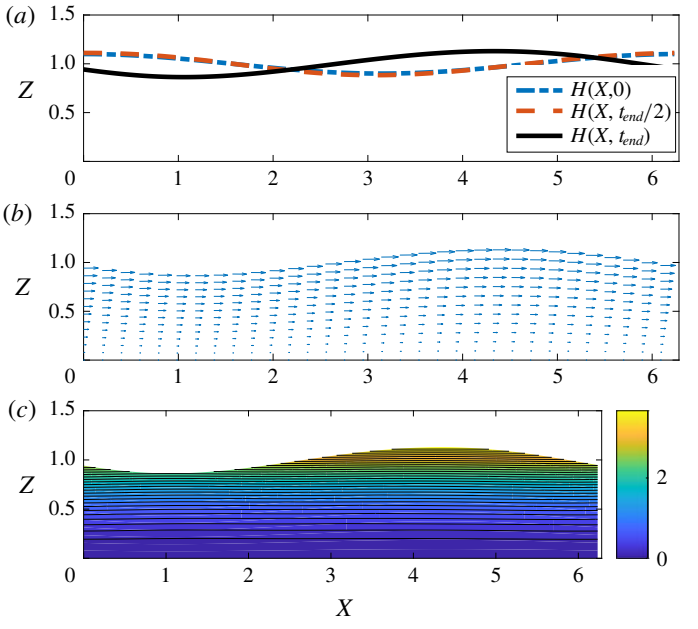


FIGURE 5. (Colour online) A strong surface shear $\tau = 6$ (vanishing odd viscosity $\eta^o/\eta^e \equiv 0$) suppresses the thermocapillary instability by inducing a permanent nonlinear viscous capillary wave on the liquid–gas interface. Numerical solutions of the evolution equation (3.15) with surface tension gradient Σ_X from (3.14). (*a*) Snapshots of the wave profiles of the liquid–gas interface. (*b*) Velocity field at time t_{end}. (*c*) Streamlines at time t_{end}.

A wide range of values of the viscosity ratio versus the thickness of the film for two different liquids is displayed in figure 8 from (5.16). For the silicon oil with values taken from table 1 with film thickness $h = 10^{-4}$ cm and $\Delta\vartheta = 20\,^{\circ}$C we find $\lambda = 0.36$ cm, k_{cr}(dimensional) $= 24$ cm^{-1}, $\epsilon = 0.0017$, $U_0 = 10$ cm s^{-1} and $\eta^o/\eta^e \sim 0.8$.

Equation (2.37),

$$H_T + \tau H H_X + \left[\frac{1}{2}\Sigma_X H^2 - \frac{1}{3}\left(\frac{\eta^o}{\eta^e}\Sigma_{XX} + G H_X - \bar{C}^{-1} H_{XXX}\right) H^3\right]_X = 0, \tag{5.20}$$

was solved numerically with periodic boundary conditions in a spatial domain of length corresponding to the wavenumber k_{cr} from (4.2) and initial condition $H(X, 0) = 1 + 0.1\cos(k_{cr}X)$. Here, Σ_X is given by (3.14). We have performed standard pseudospectral Fourier computations in conjunction with one of MatLab's variable time-stepping routines (Shampine & Reichelt 1997). We found that 128 nodes were sufficient to provide the sought spatial resolution. Following Kerchman & Frenkel (1994) we performed appropriate dealiasing. This is done by setting the Fourier coefficients of H, and its derivatives corresponding to those high wavenumbers, equal to zero at each time-step and prior to calculating the nonlinear terms in physical space.

For values of the dimensionless variables $G = 3$, $\bar{C} = 1/3$, $B = 0.1$ and $M = 4(B+1)^2/B$ the time variation of the liquid–gas interface $H(X, T)$ for $(\tau, \eta^0) = (6, 0)$, $(\tau, \eta^0) = (0, 3\eta^e)$ and $(\tau, \eta^0) = (2, 2\eta^e)$ is displayed in figures 5(*a*), 6(*a*) and 7(*a*) respectively. In all cases stabilization has been reached.

https://doi.org/10.1017/jfm.2019.644 Published online by Cambridge University Press

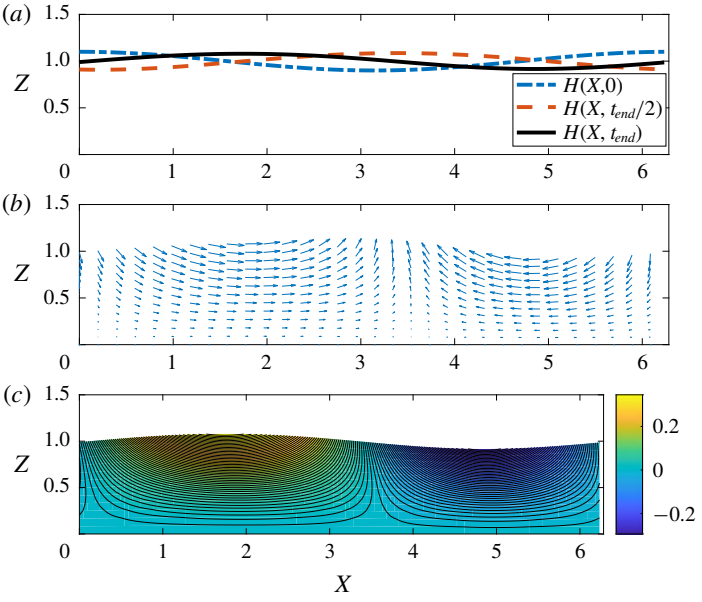


FIGURE 6. (Colour online) A non-zero odd viscosity, $\eta^o/\eta^e = 3$ (vanishing surface shear $\tau \equiv 0$), suppresses the thermocapillary instability by inducing a permanent nonlinear dispersive capillary wave on the liquid–gas interface. Numerical solutions of the evolution equation (3.15) with surface tension gradient Σ_X from (3.14). (*a*) Snapshots of the wave profiles of the liquid–gas interface. (*b*) Velocity field at time t_{end}. (*c*) Streamlines at time t_{end}.

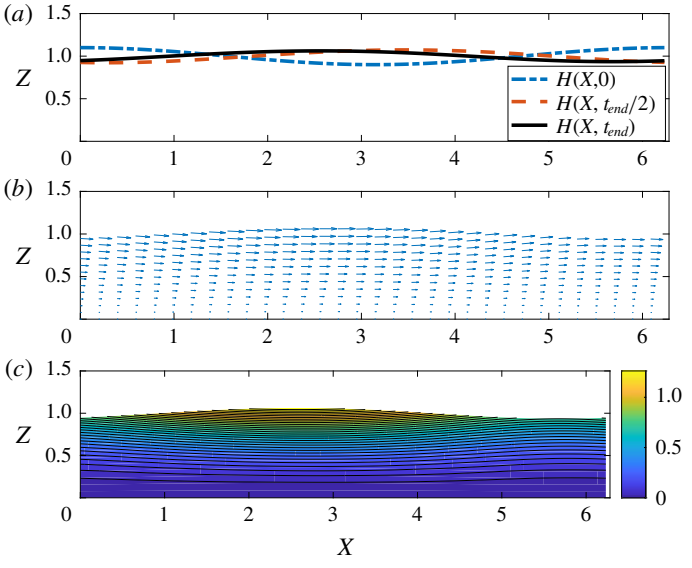


FIGURE 7. (Colour online) A non-zero odd viscosity, $\eta^o/\eta^e = 2$, and non-zero surface shear $\tau = 2$ suppress the thermocapillary instability by inducing a permanent nonlinear dispersive capillary wave on the liquid–gas interface. Numerical solutions of the evolution equation (3.15) with surface tension gradient Σ_X from (3.14). (*a*) Snapshots of the wave profiles of the liquid–gas interface. (*b*) Velocity field at time t_{end}. (*c*) Streamlines at time t_{end}.

https://doi.org/10.1017/jfm.2019.644 Published online by Cambridge University Press

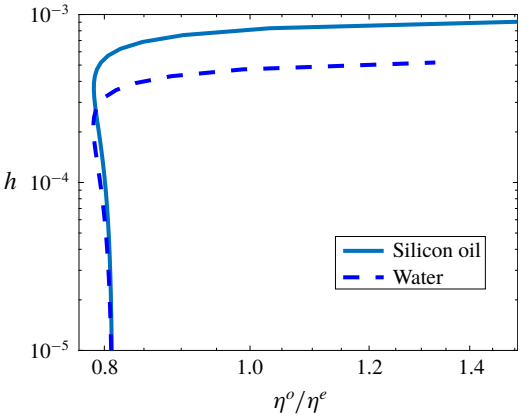


FIGURE 8. (Colour online) Plot of the critical value of the viscosity ratio η^o/η^e from (5.16) versus the dimensional film thickness h for $\Delta\vartheta = 20\,^{\circ}\mathrm{C}$ and the two liquids whose natural properties appear in table 1.

6. Discussion

In this article we have examined the effect that odd viscosity has on the motion of a thin liquid film sitting on a solid substrate and surrounded by an ambient gas phase. New terms arise in the evolution equation of the liquid–gas interface that depend on odd viscosity. The free interface can support nonlinear viscous capillary waves that become prominent only when the surface shear stress at the liquid–gas interface is spatially dependent. We demonstrate this capacity of odd viscosity liquids by resorting to a thermocapillary system whose surface shear stress is spatially-dependent. Nonlinear wave propagation is possible because the surface tension gradient breaks the reflection symmetry of the evolution equation for the liquid–gas interface. Our main result is that for a certain regime of the ratio of viscosities the incipient surface wave propagation suppresses the thermocapillary instability.

The work discussed in this article can be expanded in a number of ways whenever surface shear stresses are spatially dependent. One such instance arises naturally in a liquid with rotational degrees of freedom, for example in a magnetic liquid, see Kirkinis (2017). It also arises when one considers surface-active agents. In this case the surface tension gradient is proportional to the gradient of the adsorbed concentration, see for instance Oron *et al.* (1997).

Acknowledgements

The authors are grateful to three anonymous referees for their suggestions and criticism that significantly improved the manuscript. This work was supported by the US Department of Energy Office of Science, Basic Energy Sciences under Award no. DE-FG02-07ER46452.

Appendix A. Constitutive relations in the presence of a magnetic field

A magnetic field breaks the time-reversal symmetry and endows a liquid with an odd viscosity coefficient. In general the viscous stress tensor is of the form (Lifshitz & Pitaevskii 1981, § 13)

$$\sigma'_{\alpha\beta} = \eta_{\alpha\beta\gamma\delta} V_{\gamma\delta}, \tag{A 1}$$

https://doi.org/10.1017/jfm.2019.644 Published online by Cambridge University Press

where $V_{\gamma\delta}=\frac{1}{2}((\partial u_\gamma/\partial x_\delta)+(\partial u_\delta/\partial x_\gamma))$. With the notation $\boldsymbol{b}=\boldsymbol{B}/B$ for the unit vector in the direction of the magnetic field $\boldsymbol{B}$ and for an incompressible liquid the viscous stress tensor is expressed in the form

$$\begin{aligned}\sigma'_{\alpha\beta} \;=\; & 2V_{\alpha\beta}(\eta+\eta_1)+V_{\beta\gamma}[2(\eta_2-\eta_1)b_\gamma b_\alpha+\eta_3 b_{\alpha\gamma}]+V_{\alpha\gamma}[2(\eta_2-\eta_1)b_\gamma b_\beta+\eta_3 b_{\beta\gamma}]\\ & +V_{\gamma\delta}[(\eta_1+\zeta_1)\delta_{\alpha\beta}b_\gamma b_\delta+(\eta_1-4\eta_2)b_\alpha b_\beta b_\gamma b_\delta+(2\eta_4-\eta_3)(b_{\alpha\gamma}b_\beta b_\delta+b_{\beta\gamma}b_\alpha b_\delta)],\end{aligned} \tag{A 2}$$

where $b_{\alpha\beta}=\epsilon_{\alpha\beta\gamma}b_\gamma$ and η_i, ζ_i are viscosity coefficients. For the geometry considered in this article and for a magnetic field in the y-direction, setting $b_2=b$ and considering the long-wavelength approximation we obtain

$$\sigma_{13}=\sigma_{31}=(\eta+\eta_1)u_z, \quad \sigma_{33}=-\sigma_{11}=\eta_3 b u_z. \tag{A 3a,b}$$

Comparing these expressions with (2.4) leads to the identification $\eta^o\equiv\eta_3 b$.

The heat flux $\boldsymbol{q}$, in the presence of a magnetic field, becomes (Lifshitz & Pitaevskii 1981, § 13)

$$\boldsymbol{q}=-k_{th}\boldsymbol{\nabla}\vartheta-\kappa_1\boldsymbol{b}(\boldsymbol{b}\cdot\boldsymbol{\nabla}\vartheta)-\kappa_2\boldsymbol{\nabla}\vartheta\times\boldsymbol{b}, \tag{A 4}$$

for the thermal conductivities k_{th} and κ_i. With respect to the conditions mentioned above, the two components of $\boldsymbol{q}$ become

$$q_1=-k_{th}\vartheta_x+\kappa_2 b\vartheta_z \quad \text{and} \quad q_3=-\kappa_2 b\vartheta_x-k_{th}\vartheta_z, \tag{A 5a,b}$$

so that

$$-\mathrm{div}\boldsymbol{q}=k_{th}\vartheta_{xx}-\kappa_2 b\vartheta_{xz}+\kappa_2 b\vartheta_{zx}+k_{th}\vartheta_{zz}. \tag{A 6}$$

Thus, in the long-wavelength limit, only the last term on the right-hand side of (A 6) is of order one and this recovers the energy equation (3.7). Similarly, the boundary condition $\boldsymbol{n}\cdot\boldsymbol{\nabla}\boldsymbol{q}=\alpha_{th}(\vartheta-\vartheta_\infty)$ at the liquid–gas interface reduces to (3.8).

Appendix B. Non-dissipative nature of odd viscosity: absence of viscous heating

An alternative argument to the existing ones regarding the non-dissipative nature of odd viscosity is that it does not raise the temperature of a liquid. From Landau & Lifshitz (1987) equation (50.1) we know that the energy equation of a moving liquid with heat conduction and viscous heating is

$$\rho c_p(\vartheta_t+\boldsymbol{u}\cdot\mathrm{grad}\vartheta)=k\nabla^2\vartheta+\sigma'_{ik}\frac{\partial u_i}{\partial x_k}, \tag{B 1}$$

where

$$\sigma'_{ik}=\eta^e\left(\frac{\partial u_i}{\partial x_k}+\frac{\partial u_k}{\partial x_i}\right)+\sigma^o_{ik}, \tag{B 2}$$

(see (2.2) and (2.3)). Employing expression (2.3) for the odd part of the stress tensor and after some rearrangement and symmetrization (B 1) becomes

$$\rho c_p(\vartheta_t+\boldsymbol{u}\cdot\mathrm{grad}\vartheta)=k\nabla^2\vartheta+\frac{\eta^e}{2}\left(\frac{\partial u_i}{\partial x_k}+\frac{\partial u_k}{\partial x_i}\right)^2, \tag{B 3}$$

which shows that only the part of the stress tensor associated with the even viscosity can raise the temperature of a liquid. One would expect this result also on the basis

https://doi.org/10.1017/jfm.2019.644 Published online by Cambridge University Press

of vanishing surface terms (that contain the pressure multiplied by velocity) in the energy equation. See equation (16.2) of Landau & Lifshitz (1987).

Following the same line of arguments one can show that the evolution of the entropy in a liquid with heat conduction is also not affected by odd viscosity, whether the liquid is incompressible or not, see equations (49.4) and (49.5) in Landau & Lifshitz (1987).

Still the same arguments lead to the conclusion that energy dissipation leads to a decrease in mechanical energy (cf. equation (16.3) in Landau & Lifshitz (1987))

$$\dot{E}_{\rm kin} = -\frac{1}{2}\eta^e \int \left(\frac{\partial u_i}{\partial x_k} + \frac{\partial u_k}{\partial x_i}\right)^2 {\rm d}^3x, \tag{B 4}$$

so that the even coefficient of viscosity is always positive.

Appendix C. Derivation of the Landau equation

To understand the logic behind the bifurcation criterion (5.12) we return to our discussion of § 5.2 and derive the Landau equation. Expand H about a steady state

$$\begin{aligned} H \;=\; & 1 + \delta[A_1(\delta^2 T){\rm e}^{{\rm i}q(X-VT)} + A_1^*(\delta^2 T){\rm e}^{-{\rm i}q(X-VT)}] \\ & + \delta^2[A_2(\delta^2 T){\rm e}^{2{\rm i}q(X-VT)} + A_2^*(\delta^2 T){\rm e}^{-2{\rm i}q(X-VT)}] + O(\delta^3), \end{aligned} \tag{C 1}$$

for complex amplitudes A_1, A_2 etc. where V is given by (5.11*a*). Introduce the bifurcation parameter

$$\mu = \frac{M - M_{cr}}{M_{cr}} \tag{C 2}$$

and expand in δ so that $\mu = \mu_0 + \delta^2\mu_2 + \cdots$. This means that the expansion parameter δ is defined by

$$\delta^2 = \frac{\mu - \mu_0}{\mu_2}. \tag{C 3}$$

The slow time dependence $\delta^2 T$ is suggested by the linearized theory indicating that the amplitude of the critical mode is a function of $|M - M_{cr}|T$ as $|M - M_{cr}| \to 0$ (Erneux & Davis 1993).

In (3.15) we set $\tau \equiv 0$ to simplify the presentation. Substituting (C 1) into (3.15) leads to a Landau equation for the amplitude A_1. Setting $A_1 = R{\rm e}^{{\rm i}\varphi}$ and solving for the real part of the Landau equation we obtain

$$\begin{aligned} \frac{{\rm d}R}{{\rm d}\hat{T}} \;=\; & \frac{\mu_2 q^2 G}{3} R + \frac{q^2}{18\bar{C}\left(9\,q^2 + (\bar{C}G + q^2)^2\left(\dfrac{\eta^o}{\eta^e}\right)^2\right)(B+1)^2} \\ & \times \left(2(\bar{C}G + q^2)^2(27B^2\bar{C}G + 35B^2q^2 + 42B\bar{C}G + 30Bq^2 + 12\bar{C}G - 24q^2)\left(\frac{\eta^o}{\eta^e}\right)^2\right. \\ & \left. + 9(\bar{C}G + q^2)(9B^2\bar{C}G + 45B^2q^2 + 6B\bar{C}G + 30Bq^2 + \bar{C}G + 7q^2)\right) R^3. \end{aligned} \tag{C 4}$$

Equation (C 4) is of the general form

$$\frac{{\rm d}R}{{\rm d}\hat{T}} = \alpha R - \beta R^3, \tag{C 5}$$

https://doi.org/10.1017/jfm.2019.644 Published online by Cambridge University Press

where the coefficients α and β can be read off from (C 4) and $\hat{T} = \delta^2 T$. When the parameters α and β are positive (equivalently when the bifurcation parameter a_2 in (5.12) is positive), the Landau equation acquires the (stable) steady-state solution

$$R = \sqrt{\frac{\alpha}{\beta}}, \tag{C 6}$$

observed in the numerical simulations. When $a_2 < 0$ no such steady-state solutions exist. The equivalence between the right-hand side of (C 4) and (5.12) can be established by setting $R = \sqrt{A_c^2 + A_s^2}/2$.

REFERENCES

ABANOV, A., CAN, T. & GANESHAN, S. 2018 Odd surface waves in two-dimensional incompressible fluids. *SciPost Physics* **5** (1), 010.

AVRON, J. E. 1998 Odd viscosity. *J. Stat. Phys.* **92** (3–4), 543–557.

BANERJEE, D., SOUSLOV, A., ABANOV, A. G. & VITELLI, V. 2017 Odd viscosity in chiral active fluids. *Nat. Commun.* **8** (1), 1573.

CHAVES, A., ZAHN, M. & RINALDI, C. 2008 Spin-up flow of ferrofluids: asymptotic theory and experimental measurements. *Phys. Fluids* **20** (5), 053102.

CROSS, M. C. & HOHENBERG, P. C. 1993 Pattern formation outside of equilibrium. *Rev. Mod. Phys.* **65** (3), 851–1112.

DAVIS, M. J., GRATTON, M. B. & DAVIS, S. H. 2010 Suppressing van der Waals driven rupture through shear. *J. Fluid Mech.* **661**, 522–539.

DAVIS, S. H. 1987 Thermocapillary instabilities. *Annu. Rev. Fluid Mech.* **19** (1), 403–435.

DAVIS, S. H. 2002 Interfacial fluid dynamics. In *Perspectives in Fluid Dynamics: A Collective Introduction to Current Research* (ed. G. K. Batchelor, H. K. Moffatt & M. G. Worster), pp. 1–51. Cambridge University Press.

ERNEUX, T. & DAVIS, S. H. 1993 Nonlinear rupture of free films. *Phys. Fluids* A **5** (5), 1117–1122.

GANESHAN, S. & ABANOV, A. G. 2017 Odd viscosity in two-dimensional incompressible fluids. *Phys. Rev. Fluids* **2** (9), 094101.

KATAOKA, D. E. & TROIAN, S. M. 1999 Patterning liquid flow on the microscopic scale. *Nature* **402** (6763), 794–797.

KAWAHARA, T. 1983 Formation of saturated solitons in a nonlinear dispersive system with instability and dissipation. *Phys. Rev. Lett.* **51** (5), 381–383.

KAWAHARA, T. & TOH, S. 1988 Pulse interactions in an unstable dissipative-dispersive nonlinear system. *Phys. Fluids* **31** (8), 2103–2111.

KERCHMAN, V. I. & FRENKEL, A. L. 1994 Interactions of coherent structures in a film flow: simulations of a highly nonlinear evolution equation. *Theor. Comput. Fluid Dyn.* **6** (4), 235–254.

KIRKINIS, E. 2017 Magnetic torque-induced suppression of van-der-Waals-driven thin liquid film rupture. *J. Fluid Mech.* **813**, 991–1006.

KIRKINIS, E. & DAVIS, S. H. 2015 Stabilization mechanisms in the evolution of thin liquid-films. *Proc. R. Soc. Lond.* A **471**, 20150651.

KIRKINIS, E. & ANDREEV, A. V. 2019 Healing of thermocapillary film rupture by viscous heating. *J. Fluid Mech.* **872**, 308–326.

LANDAU, L. D. & LIFSHITZ, E. M. 1987 *Fluid Mechanics. Course of Theoretical Physics*, vol. 6. Pergamon.

LAPA, M. F. & HUGHES, T. L. 2014 Swimming at low Reynolds number in fluids with odd, or hall, viscosity. *Phys. Rev.* E **89** (4), 043019.

LIFSHITZ, E. M. & PITAEVSKII, L. P. 1981 *Course of Theoretical Physics. Vol. 10: Physical Kinetics*, Butterworth Heinemann.

https://doi.org/10.1017/jfm.2019.644 Published online by Cambridge University Press

MAGGI, C., SAGLIMBENI, F., DIPALO, M., DE ANGELIS, F. & DI LEONARDO, R. 2015 Micromotors with asymmetric shape that efficiently convert light into work by thermocapillary effects. *Nat. Commun.* **6**, 7855.

ORON, A., DAVIS, S. H. & BANKOFF, S. G. 1997 Long-scale evolution of thin liquid films. *Rev. Mod. Phys.* **69** (3), 931–980.

SHAMPINE, L. F. & REICHELT, M. W. 1997 The matlab ode suite. *SIAM J. Sci. Comput.* **18** (1), 1–22.

SUMINO, Y., NAGAI, K. H., SHITAKA, Y., TANAKA, D., YOSHIKAWA, K., CHATÉ, H. & OIWA, K. 2012 Large-scale vortex lattice emerging from collectively moving microtubules. *Nature* **483** (7390), 448–452.

TAN, M. J., BANKOFF, S. G. & DAVIS, S. H. 1990 Steady thermocapillary flows of thin liquid layers. I. Theory. *Phys. Fluids* A **2** (3), 313–321.

TSAI, J.-C., YE, F., RODRIGUEZ, J., GOLLUB, J. P. & LUBENSKY, T. C. 2005 A chiral granular gas. *Phys. Rev. Lett.* **94** (21), 214301.

https://doi.org/10.1017/jfm.2019.644 Published online by Cambridge University Press